ELSEVIER

Biochimica et Biophysica Acta 1195 (1994) 11–20

BBA Biochimica et Biophysica Acta

Poly(ethylene glycol) on the liposome surface: on the mechanism of polymer-coated liposome longevity

Vladimir P. Torchilin [a,*], Vladimir G. Omelyanenko [b], Mikhail I. Papisov [c], Alexei A. Bogdanov, Jr. [c], Vladimir S. Trubetskoy [a], James N. Herron [b], Christine A. Gentry [b]

[a] *Center for Imaging and Pharmaceutical Research, Massachusetts General Hospital-East, 149 13th Street, Charlestown, MA 02129, USA*
[b] *Department of Pharmaceutics, University of Utah, Salt Lake City, UT 84108, USA*
[c] *MGH-NMR Center, Department of Radiology, Massachusetts General Hospital-East, Charlestown, MA 02129, USA*

Received 15 March 1994

Abstract

The hypothetical model is built explaining the molecular mechanism of protective action of poly(ethylene glycol) on liposomes in vivo. The protective layer of the polymer on the liposome surface is considered as a statistical 'cloud' of polymer possible conformations in solution. Computer simulation was used to demonstrate that relatively a small number of liposome-grafted molecules of hydrophilic and flexible polymer can create a dense protective conformational cloud over the liposome surface preventing opsonizing protein molecules from contacting liposome. A more rigid polymer fails to form this dense protective cloud, even when hydrophilic. Computer simulation was also used to reveal possible heterogeneity of reactive sites on a polymer-coated liposome surface, and to estimate the optimal polymer-to-lipid ratio for efficient liposome protection. Experiments have been performed with the quenching of liposome-associated fluorescent label (nitrobenzoxadiazole or fluorescein) with protein (rhodamine-ovalbumin or anti-fluorescein antibody) from solution. It was shown that poly(ethylene glycol) grafting to liposomes hinders protein interaction with the liposome surface, whereas liposome-grafted dextran (more rigid polymer) in similar quantities does not affect protein–liposome interaction. Highly-reactive and low-reactive populations of chemically identical reactive sites have been found on polymer-coated liposomes. Experimental data satisfactory confirm the suggested mechanism for the longevity of polymer-modified liposome.

Keywords: Long-circulating liposome; Liposome; Poly(ethylene glycol); Computer simulation; Fluorescence quenching; Anti-fluorescein antibody

1. Introduction

The most important drawback of liposomes as potential drug carriers [1] is their fast clearance from the circulation and uptake by the cells of the reticulo-endothelial system (RES). Liposome recognition and uptake occurs, primarily, in liver and spleen, and are believed to be the result of fast liposome opsonization in the blood [2]. To target liposomal pharmaceuticals to organs other than the liver and spleen, liposomes have been modified with specific targeting moieties (antibodies) [3]. However, immunoliposomes also do not exhibit prolonged circulation and fail to accumulate sufficiently in the targets with diminished blood supply or/and low antigen concentration when increased circulation times for liposome–target interaction are required. Numerous attempts have been made to prolong liposome lifetime in the circulation, using such methods as varying of the liposome size [4], coating liposomes with some plasma proteins [5], and RES blockade by presaturation with 'empty' liposomes [6].

Abbreviations: PEG, poly(ethylene glycol); PE, phosphatidylethanolamine; PEG-OSu, monometoxy-PEG-succinimidyl succinate; SA, sterylamine; NBD, *N*-(7-nitrobenz-2-oxa-1,3-diazol-4-yl); NBD-PE, NBD-dioleoylphosphatadylethanolamine; Rh, sulforhodamine; Rh-OVA, Rh-ovalbumin conjugate; GFl, *N*-[glutarylamido-(5-amidoacetamido-fluorescein)]; GFl-PE, GFl-1,2-dioleoyl-*sn*-glycero-3-phosphoethanolamine.

* Corresponding author. Fax: +1 (617) 7267830.

SSDI 0005-2736(94)00155-I

An important breakthrough in this field was achieved when long-circulating liposomes were first described [7–9]. One of the more general methods of preparation involves liposome coating with PEG [10–12], leaving the molecular mechanism of PEG action obscure. The explanation of this phenomenon involves the participation of PEG in the repulsive interactions between PEG-grafted membranes and another particles [13], the role of surface charge and hydrophilicity of PEG-coated liposomes [14], and generally speaking, the decreased rate of plasma proteins (opsonins) adsorption on the hydrophilic surface of PEGylated liposomes [15].

In an attempt to explain what peculiarities of PEG behavior on the liposome surface underlay its ability to prevent liposome opsonization, we hypothesized that the molecular mechanism of PEG protective action is determined by the properties of a flexible polymer molecule (free rotation of individual units around inter-unit linkages) in solution, and includes the formation of dense polymeric 'cloud' over the liposome surface even at relatively low polymer concentrations [16]. Here, we would like to describe further the development of our hypothesis including the computer simulation of the model, and submit the first experimental support for it. Our investigations have also lead us to conclude that optimal PEG concentration for the preparation of long-circulating liposomes and immunoliposomes can be predicted as well as optimal PEG molecular weight.

2. Materials and methods

2.1. Computer simulation

Spatial distribution of short polymers grafted onto the liposome surface was simulated using a three-dimensional random flight model. The polymer was assumed to consist of absolutely rigid segments with free segment rotation around intersegmental conjunction. The program developed, using MSExcel macrolanguage for the computer simulation of random polymer conformation, included following procedures.

Before the calculation, the grafting point was assumed to be located at $x = y = z = 0$. At step one, the random direction of the first segment was assumed by generation of two random angles: between the segment axis and axis z, and between the segment axis projection onto xy plain and axis x. At step two, the coordinates of the remote end of the first segment were calculated, conditionally assuming segment length $l = 1$ nm for a flexible polymer and $l = 5$ nm for a rigid one. If the resulting position of the segment terminus was invalid (segment location below the liposome surface, i.e., $z < 0$), the result was omitted. Steps one and two were repeated until the segment terminus was positioned above the liposome surface. Then, the resulting coordinates were used as a starting point for the calculation of the next segment position following the same procedure.

The arrays of segment terminus coordinates were used to illustrate grafted polymer conformations, and to calculate the relative polymer density over the liposome surface. In this model, the segment mass is assumed to concentrate at the remote segment terminus. This assumption distorts the profile of mass distribution for the very first segment. The distribution of segments, starting from the third one, is practically insensitive to this assumption (test results not shown).

Corresponding to our model, the degree of the liposome surface protection by polymer molecule should correlate with the effective polymer density per surface square unit. To gain insight into the possible pattern of surface density (i.e., the shape of the polymer 'umbrella'), the relative polymer densities for the flexible and rigid polymers were calculated. First, the distance (r) between the segment end and axis z was calculated for each segment. Then, the number of segment termini located within certain distance interval (r, $r + \Delta r$) was counted for a large number of conformations. The resulting distribution was normalized per square, i.e., divided by the area of the circular annulus of the width Δr and the inner radius equal to r. The illustrations in this article were produced using 440 simulated random conformations of each polymer (8800 segment terminus spatial coordinates).

2.2. Preparation of fluorescent labels

Fluorescent phospholipid, NBD-PE, used for incorporation into the liposome membrane was obtained from Avanti Polar Lipids. Conjugate for liposomal NBD-PE quenching was prepared from mannose-free ovalbumin (Sigma) and Lissamine™ rhodamine B sulfonyl chloride (Molecular Probes) according to manufacturer's instructions. The resultant purified Rh-OVA contained 10–15 sulforhodamine B residues per mol of protein.

Membranotropic derivative of fluorescein, GFl-PE, was synthesized from (5-aminoacetamido)fluorescein and *N*-glutaryl-dioleoyl-PE (NGPE). NGPE (19 μmol) prepared as in [17], was suspended in 1 ml of water, and 10 mg of *N*-hydroxysulfosuccinimide together with 10 mg of 1-ethyl-3-[3′-(dimethylamino)propyl]carbodiimide were added to the suspension. The reaction mixture was supplemented with 10 mg of (5-aminoacetamido)fluorescein in 0.1 M Hepes (pH 9.0). The reaction proceeded with stirring for 1 day. The product was applied on a Kieselgel 60 column in chloroform, and the column was washed with chloroform and, sequen-

tially, with 50 ml of 10% methanol in chloroform, 20% methanol, 40% methanol (lipid fraction eluted), and 60% methanol. The fraction containing lipids was concentrated by evaporation.

2.3. Anti-fluorescein antibody

Anti-fluorescein monoclonal antibody 4-4-20 able to quench fluorescein fluorescence was generated through chemically mediated fusion of BALB/c murine splenic lymphocytes with the Sp 2/0-Ag 14 myeloma cell line as described in [18]. Hybridoma cell line was obtained from Prof. Edward W. Voss, Jr., University of Illinois at Urbana-Champaign. Monoclonal antibody has been purified by ammonium sulfate precipitation, DEAE-cellulose anion exchange chromatography, and chromatofocusing over a pH gradient of 7.0 to 5.0. Antibody preparation was characterized by gel electrophoresis and fluorescein quenching assays [19]. Before use, antibody solution was filtered through Durapore 0.2 μm filters (Millipore).

2.4. Synthesis of PEG-PE and dextran-stearylamine (dextran-SA)

The synthesis of PEG-PE (PEG MW 5000) was performed as described in [10]. Briefly, an aliquot of PEG-OSu (Sigma) was added to a solution of PE (Avanti Polar Lipids) in chloroform, followed by addition of triethylamine (PEG-OSu/PE/triethylamine = 3:1:3.5, mol/mol). The reaction mixture was incubated overnight at room temperature and chloroform was evaporated with a stream of nitrogen gas. The reaction mixture was redissolved in 0.145 M NaCl. Unreacted PEG-OSu is rapidly hydrolyzed in the aqueous media. The resulting mixture in saline was applied to a Bio-Gel A-1.5m column equilibrated with saline. Peak fractions containing PEG-PE micelles eluted in the void volume were pooled, dialyzed against water and lyophilized.

Dextran-SA was prepared by reductive amination [20]. For this purpose linear dextran (Fluka, 300 mg, MW 6000), SA (Sigma, 67 mg), and sodium cyanoborohydride (Sigma, 60 mg) were dissolved in 7 ml of tetrahydrofuran/water (30:12, vol/vol) mixture and incubated for 3 weeks at 40°C with stirring. The precipitate formed was extensively washed with chloroform and than with water in order to remove unreacted stearylamine and dextran. The remaining residue was dissolved in tetrahydrofuran/water (36:10, vol/vol) mixture, and passed through Sephadex LH-20 column using the same solvent. After freeze-drying the yield of dextran-SA was found to be 105 mg.

Both PEG-PE and dextran-SA molecules contain single terminal hydrophobic residue.

2.5. Liposome preparation

Liposomes were prepared from the mixture of phosphatidyl choline and cholesterol in 7:3 molar ratio by detergent (octyl glucoside) dialysis method [21]. When necessary, 1% mol of the fluorescent label, NBD-PE or GFl-PE, or/and required quantities of PEG-PE or dextran-SA were added to the starting lipid composition. Liposomal suspensions formed were sized by consecutive filtration through 0.6, 0.4 and 0.2 μm polycarbonate filters (Nuclepore). According to the data of liposome size measurements using Coulter N4 MD Submicron Particle Size Analyzer (Coulter Electronics), all the liposome obtained were within 160 ± 25 nm range (unilamellar vesicles). For fluorescence quenching experiments liposome preparations (5 mg total lipid/ml) were diluted until it reached the required fluorescence intensity.

2.6. Fluorescence measurements

Fluorescence intensity measurements were made using a photon-counting spectrofluorimeter PC-1 (ISS). In the case of liposomal NBD quenching with Rh-OVA, 1 ml of NBD-containing liposomes (1 μM concentration as total lipid) in 50 mM phosphate buffer, 0.14 M NaCl (pH 7.5) was added into 2 ml thermostated cuvette under with stirring, and initial sample fluorescence was recorded at 25°C. Various quantities of 1 mM Rh-OVA solution in phosphate-buffered saline were then added into cuvette with stirring, and the residual fluorescence was registered after 10 min incubation. When more than 5% vol of Rh-OVA solution was added to liposome suspension, dilution factor was taken into account. To study energy transfer from liposomal NBD to OVA-bound Rh, we have used the same conditions, with the exception that total lipid concentration was 2 μM, and total quantity of Rh-OVA solution added to 1 ml of the liposomal suspension was 300 μl. Both NBD and Rh were excited at 485 nm. The emission was monitored using a monochromator with a 2 mm slit (16 nm FWHM band-pass).

Association kinetics of antifluorescein antibody with liposomal fluorescein was measured by recording the decrease in the fluorescence intensity of the fluoresceyl-ligand, as a function of time. Samples were excited at 485 nm using a monochromator with a 2 mm slit width, and emission was monitored through the interference filter 514.5 (Oriel). To ensure the pseudo-first order kinetics, antibodies were used in large molar excess towards liposomal fluorescein (92 and 10 nM, respectively). Usually, the volume of 0.5 ml of an appropriate antibody stock solution was added to 2 ml of the liposome suspension with stirring; both in 50 mM phosphate, 0.14 M NaCl (pH 8.0), 25°C.

Values for the fraction of free ligand (L/L_0) were calculated using the following formula [19]:

$$L/L_0 = \frac{F_t - F_\infty}{F_0 - F_\infty}$$

where L is the current free ligand concentration, L_0 the initial free ligand concentration, F_t the fluorescence intensity at a given time t, and F_0 and F_∞ are the initial and limiting fluorescence intensity values, respectively. The values for L/L_0 were plotted vs. time and analyzed by linear regression, which yielded the effective reaction rate constant (k_{eff}) from the least-squares slope. The bimolecular association constant (k_2) was determined from the effective rate constant using the equation:

$$k_2 = \frac{f_{b(\infty)}}{P} k_{eff}$$

where $f_{b(\infty)}$ is the equilibrium fraction of the liposome-bound fluoresceyl-ligand, and P is the active site concentration (twice antibody concentration since antibody molecule carries 2 binding sites). The equilibrium fraction of the bound ligand was determined using the equation:

$$f_{b(\infty)} = Q_\infty / Q_{max}$$

where Q_∞ is the fluorescence quenching value for the association reaction at equilibrium, and Q_{max} is the maximum quenching value and under the conditions used equals 0.98 [19,22]. In a general case, quenching values can be determined from the fluorescence measurements using the equation:

$$Q = (F_0 - F_t)/(F_0 - F_{bkg})$$

where $F_{bkg} = F_0/2$ (assuming fluorescein symmetrical distribution between outer and inner monolayers and taking into account intraliposomal fluorescein).

3. Results and discussion

3.1. Model of PEG behavior on the liposome surface

The hypothesis on the possible mechanism of PEG behavior on the liposome surface was suggested by us in [16]. Here, we present the results of the computer analysis of the model proposed.

The role of polymer chain flexibility

Liposome elimination from the blood proceeds mainly via liposome recognition by phagocytic cells, mediated by plasma opsonins adsorption onto the liposome surface [2]. The most evident approach to slow down the liposome clearance is, therefore, to prevent plasma protein contacts with the membrane. To perform our analysis of this approach, we are assuming that (i) protecting polymer is randomly distributed over the liposome surface and does not form any aggregates or clasters, (ii) there are no interactions between single polymer molecule and surrounding polymer molecules, (iii) protecting polymer contacts with plasma proteins do not result in the opsonization, and (iv) polymer itself does not contain any cell-specific moieties and does not enhance liposome capture by cells. PEG may serve as a good example of such polymer [23].

We consider the diffusional movement of a protein molecule towards the liposome surface as the initial step of a protein–liposome interaction. The degree of liposome protection can be described as the probability for the protein to collide with a polymer instead of

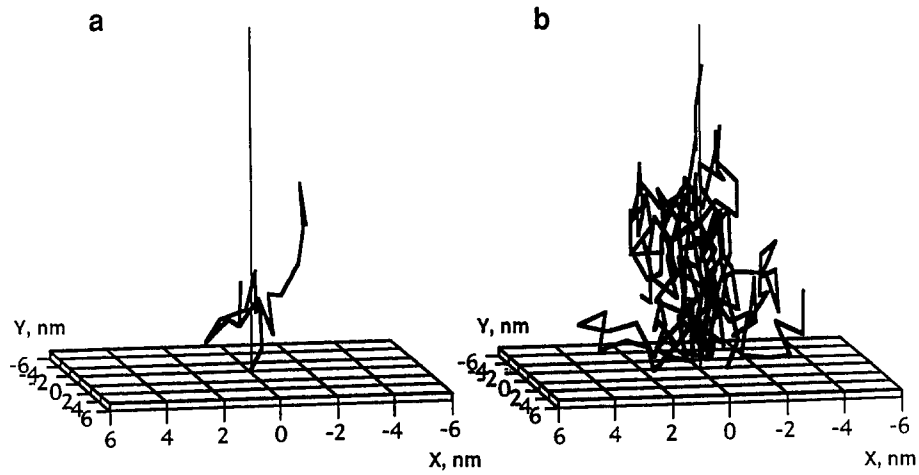

Fig. 1. Computer simulation of conformational 'cloud' formation by surface-attached polymer. Polymer molecule is conditionally assumed to consist of 20 segments, 1 nm each. Produced by random flight simulation. Unrestricted segment motion assumed. Space restriction: $Z > 0$. (a) One random conformation; (b) superposition of eleven random conformations.

liposome. We can describe the behavior of liposome-grafted polymer molecule in terms of statistical physics, e.g., applying simplified model of a polymer solution [24]. Solution can be considered as a three-dimensional network, where each cell may be occupied either with a polymer unit or with a solvent (water) molecule. The more flexible the polymer is, i.e., the more independent is the motion of any polymeric unit relative to the neighboring one, the larger the total number of its possible conformations and the higher the transition rate from one conformation to another. This means that water-soluble polymer statistically exists as a distribution ('cloud') of probable conformations. Cloud formation is illustrated in Fig. 1.

For better visual representation of the polymer density distribution, the data arrays describing conformation of the rigid polymer were produced assuming that its segment is formed of five 'frozen' segments of the flexible polymer (see Methods). Thus, the graphs of these two polymers distribution over the liposome surface (at the equal number of conformations) have equal number of points which depict polymer mass distribution. To further improve visual perception, a slice of the polymer cloud ($X = 0 \pm 0.25$ nm), rather than the entire data array, can be shown (compare Figs. 1 and 2).

Cloud density and uniformity increase with the increase of the number of possible conformations and polymer flexibility. The polymer flexibility correlates with its ability to occupy with high frequency many cells in solution, temporarily squeezing water molecules out of them (i.e., closing these cells for diffusion of other solutes). To reach the liposome surface, protein molecules have to penetrate the whole cloud formed by the liposome-attached polymer. From the computer analysis it follows (Fig. 2) that the flexible polymer forms the conformational cloud with very high density in its central part. Thus a relatively small number of water-soluble, very flexible polymer molecules can create a sufficient number of high density conformational clouds over the liposome surface, protecting the latter from opsonization and recognition. These molecules form protective 'umbrellas' on the liposome surface, and the probability value for an opsonin to meet polymer chain fragment during the diffusion towards the liposome surface will depend on the amount of surface-grafted polymer molecules and effective square of an 'umbrella' formed by single polymer molecule. This value should be maximal (maximal protection) when clouds are fused or almost fused.

As it follows from the computer simulation data, a rigid polymer of the same length (its segment was conditionally assumed to be 5-times longer than for the flexible polymer) forms a broad, but loose and thus permeable cloud. Additionally, this cloud is less uniform due to slower translocation of individual segments. Thus, even good water-solubility and hydrophilicity of a rigid polymer (such as dextran with hindered rotation of individual glucopyranosyl units around glucosidic linkages) may not provide sufficient protection for the liposome surface [25]. The number of possible conformations for such polymers is lower and the conformational transitions proceed with a slower rate than those of a flexible polymer. During a single collision act, the number of water molecules disturbed within the loose conformational cloud formed by a rigid polymer will be much smaller. It appears that there should exist a sufficient water space through which the normal diffusion of proteins toward the liposome surface can still proceed with high probability. Thus, to protect the liposome, one has to bind a much larger number of rigid polymer molecules on the liposome surface. This difference between flexible and rigid polymers may only increase with the polymer MW. Only when the same polymer combines both hydrophilicity and flexibility (like PEG), can it serve as an effective liposome protector even at relatively low concentrations on the surface. The model used allows us to suggest other possible candidates to serve as liposome-protecting polymers. Those can be, for example, soluble and flexible poly(acrylamide) and poly(vinyl pyrrolidone), provided that these polymers do not form any aggregates or clasters on the liposome surface, and

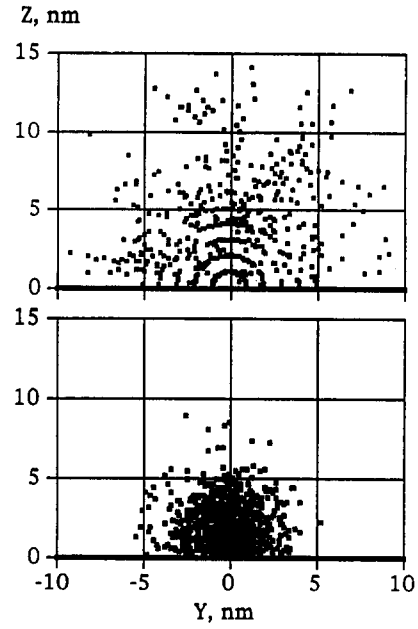

Fig. 2. Distribution of polymer conformations in space; slice $X = 0 \pm 0.25$ nm. Produced by random flight simulation ($Z > 0$, polymer length 20 nm, 440 conformations). Upper panel: segment length is 5 nm (rigid polymer); lower panel: segment length is 1 nm (flexible polymer). Calculations for the rigid polymer have been done under the assumption that only every fifth 1-nm segment may change the direction. The 'rings' on the upper panel are the result of the assumption that the net mass is concentrated at the remote termini of 'frozen' shorter segments.

do not have any specific affinity towards cells or plasma proteins. Unfortunately, terminal-modified derivatives of poly(acrylamide) and poly(vinyl pyrrolidone) are not available, and at present we are unable to try this prediction in direct experiment. However, synthesis of hydrophobically-modified polymers other than PEG, and their possible use for liposome protection are subjects of our current studies.

Two types of active sites on PEG-coated surface

If there exist any reactive centers on the liposome surface (e.g., binding sites for opsonins or immobilized targeting moieties), the presence of PEG in concentrations insufficient for complete coating of the surface should lead to the appearance of two populations of those centers. The first population will consist of reactive moieties excluded from the volume occupied by PEG. Such reactive centers should posses all the properties (including the reactivity) of similar centers on 'plain' liposomes. Other centers remaining within the polymer cloud form the second population with sharply decreased ability to participate in 'normal' interactions. Fig. 3 illustrates this phenomenon, and permits to suppose that kinetic parameters of the reactive site will depend on its location on the liposome surface partially coated with PEG. This model permits us to consider the possibility of simultaneous immobilization of protective polymer and some targeting ligand (antibody) on the liposome surface [26].

Optimal size of protective polymer molecule

The approach developed opens the opportunity to predict the optimal size (molecular weight) of protective polymer molecules (Fig. 4). The assumption that a certain minimal level of polymer cloud density (MDL) provides sufficient protection to the liposome surface, allows us to suggest the existence of polymer length optimum (Fig. 4B). Below the optimum, the polymer cloud will not have enough density even near the attachment point (Fig. 4A), whereas very long polymers provide density much above the necessary one (Fig. 4C). For these model calculations, MDL value has been chosen arbitrarily, whereas in the real situation we can easily connect it with kinetic parameters of liposome–opsonin interaction [16] or desired surface density of protecting polymer, and make a proper choice of a polymer for each particular case.

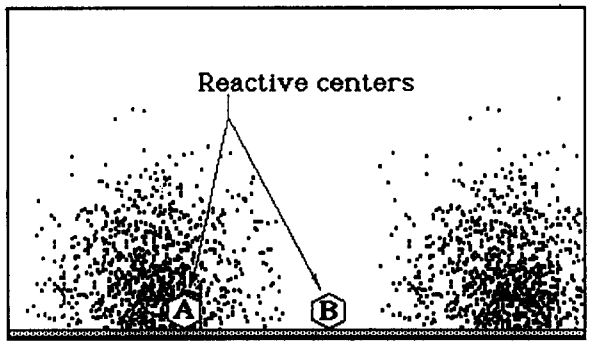

Fig. 3. The scheme of reactive site location on the liposome surface at low PEG concentration. The site can be either sterically hindered by polymer 'cloud' (A), or exposed and readily available for a variety of interactions (B). Kinetic parameters of chemically identical but differently located sites may differ.

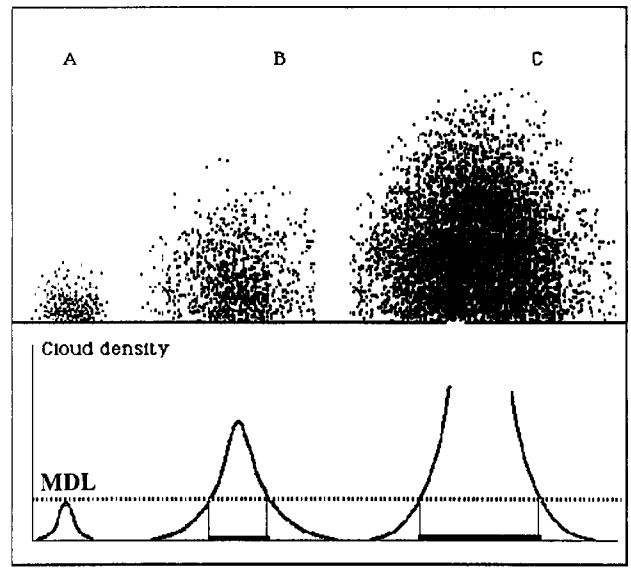

Fig. 4. Polymers of different length grafted onto the liposome surface and corresponding densities of polymer 'clouds' (non-quantitative computer simulation). MDL, minimal level of polymer 'cloud' density providing sufficient protection for the surface. A, short-chain polymer cannot create sufficiently dense 'cloud', even if it is highly flexible. B, polymer with optimal chain length provides sufficient protection and still does not exclude the possibility of surface-located reactive sites to enter normal interactions. C, polymer with excessive molecular weight provides unnecessary high 'cloud' density and sterically hinders any reactive site on the liposome surface.

Moreover, one can estimate the size of the area on the liposome surface protected with a single polymer molecule of a given molecular weight, and the number of such polymer molecules required to protect the liposome of a given size. Using the data presented in Fig. 2, one can find the radius of the 'dense cloud' for a given polymer. A polymer molecule in solution is located mainly in the volume 'between the ends' (inside the appropriate hemi-sphere for the surface-attached polymer). The end-to-end distance may be used as an estimate for the protected square radius. Combining the average end-to-end distance of a polymer (PEG) random coil in solution for PEG of various molecular weight [27] with the geometry of liposomes (the data from [28,29] give us $4.25 \cdot 10^4$ lipid molecules in the outer monolayer of 100 nm liposomes, and total surface area of $3.14 \cdot 10^4$ nm^2), we can estimate the number of PEG molecules required for 100% protection of the liposome surface with PEG of a certain

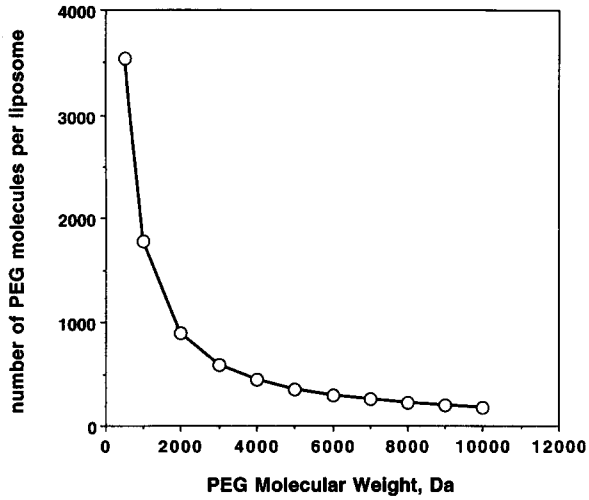

Fig. 5. The dependence of the number of PEG molecules required for complete protection of 100-nm liposome on PEG molecular weight.

molecular weight (Fig. 5). Our calculations are in good agreement with published experimental data [26,30].

3.2. Fluorescent markers on the surface of PEG-coated liposome

Quenching of NBD fluorescence with macromolecular Rh derivative

To prove our hypothesis experimentally we have investigated the efficacy of the fluorescence quenching of the liposome-incorporated NBD-PE with soluble Rh-OVA, depending on the type of the liposome-attached polymer. Preliminary results have shown that the liposomal NBD interacts with OVA-immobilized Rh. To prove this, we have obtained the fluorescence spectra of polymer-free NBD-containing liposomes in the presence of Rh-OVA, as well as the spectra of all the individual components of the system (Fig. 6). The accessibility of the liposome surface for a protein allows for the excitation energy transfer from the liposomal NBD to OVA-bound Rh. As a result, the intensity of NBD fluorescence at 530 nm decreases (compare spectra 1 and 4 on Fig. 6). At the same time, the intensity of protein-bound Rh fluorescence at 570 nm increases (compare spectra 3 and 2). The curve 5 is obtained theoretically by summarizing the fluorescence spectrum of Rh-OVA in the absence of liposomes (excitation at 485 nm), and NBD fluorescence spectrum under the condition that its maximal intensity is equal to the fluorescence intensity at 530 nm for the mixture of NBD-liposomes and Rh-OVA. The result shows that theoretical summarizing of NBD and Rh fluorescence at 570 nm (no NBD–Rh interaction, curve 5) gives noticeably lower fluorescence intensity than was obtained experimentally (spectrum 2). This finding indicates the energy transfer from the liposomal NBD to Rh and, proves liposomal NBD interaction with Rh-OVA.

To study the interaction of polymer-modified NBD-liposomes with Rh-OVA, plain NBD-liposomes and NBD-liposomes containing 1% mol of lipid-conjugated either PEG or dextran were treated with increasing quantities of Rh-OVA. NBD fluorescence diminished identically for Rh-OVA-treated 'plain' NBD-liposomes and NBD-liposomes with 1% mol of dextran (Fig. 7). About 50% of initial fluorescence can be quenched, which evidences even distribution of liposomal NBD between outer and inner monolayers of the membrane (only 'outer' NBD is susceptible for quenching). However, NBD fluorescence quenching is drastically hindered in NBD-liposomes containing 1% mol of PEG

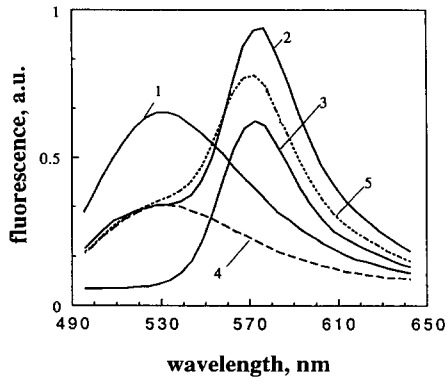

Fig. 6. The fluorescence spectra of NBD-liposomes/Rh-OVA system and its individual components. 1, NBD-liposomes; 2, the mixture of NBD-liposomes and Rh-OVA; 3, Rh-OVA; 4, NBD-liposomes when maximal fluorescence at 530 nm equals to 530 nm fluorescence for the spectrum 2; curve 5, theoretical sum of spectra 3 and 4. See experimental part for detail.

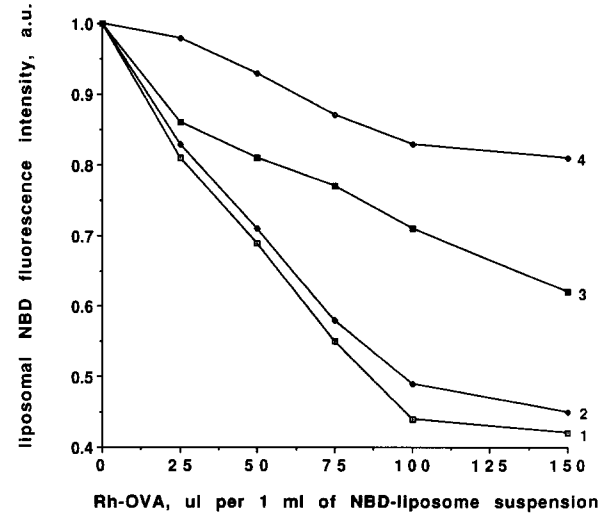

Fig. 7. Quenching of liposomal NBD fluorescence with Rh-OVA from the solution at different Rh-OVA concentrations. 1, 'plain' liposomes; 2, liposomes with 1% mol dextran-stearylamine; 3, liposomes with 0.2% mol PEG-PE; 4, liposomes with 1% mol PEG-PE. See experimental part for detail.

(theoretical quantity of PEG 5000 required for complete liposome protection, see Fig. 5). Even at maximal Rh-OVA concentration, we still observed about 80% of the initial fluorescence. The presence of 0.2% mol of PEG on the liposome surface causes much smaller decrease in fluorescence quenching, which is still far below than that for plain and dextran-coated liposomes. Since the whole quenching process is limited only by Rh-OAB diffusion from the solution to the liposome surface, it is evident that the presence of PEG on the surface creates diffusional hindrances for this process. The extent of those hindrances naturally depends on the quantity of protective polymet on the liposome surface. The data agree well with our hypothesis on different densities of 'protective clouds' for flexible (PEG) and rigid (dextran) polymers.

Interaction of anti-fluorescein antibody with liposomal fluorescein

Another experimental proof for our hypothesis was obtained using the system involving liposome surface-incorporated fluorescein, GFl-PE, and anti-fluorescein antibody (Figs. 8 and 9, Table 1). In this case Q values were equal for 'plain' GFl-liposomes and for GFl-liposomes with 1% mol of dextran, k_{eff} and k_2 values were also identical (Figs. 9A and 9C, Table 1). This indicates that the presence of dextran in the quantities used did not create any diffusional limitations for antibody–fluorescein interactions. The presence of 1% mol PEG in liposomes noticeably decreased both the rate of fluorescein quenching and the quantity of fluorescein residues accessible for the interaction with antibody (Fig. 8). The Q value was also substantially decreased (from 0.76 to 0.58), as well as both rate constants (by ca. 5-fold). This effect may be explained by strong diffusional limitations for antibody penetration towards the liposome surface imposed by PEG.

Incorporation of smaller quantity of PEG (0.2% mol) into liposomes revealed a somewhat decreased total quenching (the Q value number is intermediate between two marginal cases), and the existence of two

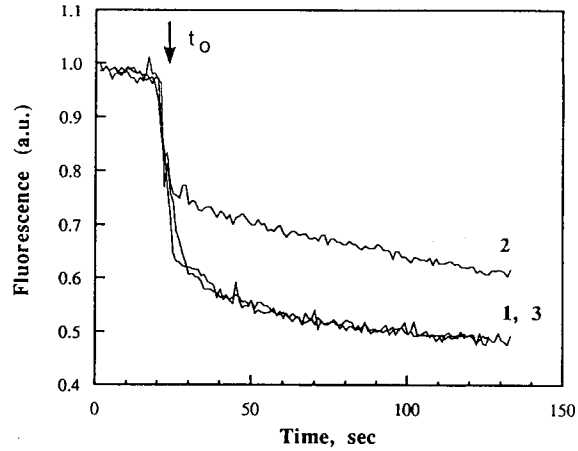

Fig. 8. Actual typical time-courses of liposomal fluorescein quenching with anti-fluorescein antibody. 1, 'plain' fluorescein-liposomes; 2, fluorescein-liposomes with 1% mol of PEG; 3, fluorescein-liposomes with 1% mol of dextran. t_o, the point of antibody addition to liposomes; this parameter can vary slightly in different runs. See experimental part for detail.

different fluorescein pools on the liposome surface (Fig. 9B). One of them was quenched with the same time rate as fluorescein on PEG-free liposomes (similar values for both kinetic constants; Table 1), whereas the quenching kinetics for another was close to that for fluorescein on PEG-liposomes with high PEG content. This can reflect different location of fluorescein molecules on the liposome surface – between and inside PEG 'clouds', as we predicted on the basis of computer simulation data (Fig. 3). Thus, the kinetic parameters of reactive site really depend on its location on the liposome surface when the quantity of PEG on the liposome is not sufficient to form an even protective cloud over the liposome surface.

In all the above experiments we have used relatively low quantity of PEG for liposome steric protection (around 1% mol) which, according to our model (see Fig. 5), can already provide even coat on liposome, but still permits some diffusion of penetrating molecules towards the liposome surface (we still observe some liposomal fluorescence quenching with both Ph-OVA and anti-fluorescein antibody). The use of higher PEG concentrations (well above MDL level) can almost completely block this diffusion, as has been shown by us [31] and others [32]. This also agrees well with our model and demonstrates the importance of the properly chosen PEG concentration for the realization of biological effects of sterically protected liposomes.

In conclusion we would like to stress the fact that the role of statistical properties of macromolecules in the solution might be decisive in PEG-coated liposome longevity in vivo. Our hypothetical assumption gained further verification by both computer simulation data and experimental results. The approach developed allows one to calculate optimal concentrations of lipo-

Table 1
Kinetic parameters of liposomal fluorescein quenching with anti-fluorescein antibody for different liposome preparations

Liposome	Q	k_{eff} (s^{-1})	k_2 ($M^{-1}s^{-1}$)
'Plain'	0.76±0.05	0.07±0.01	$2.9 \cdot 10^5$
0.2% mol PEG	0.70±0.05	0.06±0.01 [a]	$2.3 \cdot 10^5$ [a]
		0.02±0.01 [b]	$0.9 \cdot 10^5$ [b]
1% mol PEG	0.58±0.05	0.02±0.005	$0.6 \cdot 10^5$
1% mol dextran	0.76±0.05	0.07±0.01	$2.9 \cdot 10^5$

The data are given as $M \pm$S.E. for 3–6 independent measurements for each sample. See experimental part for detail.
[a] Kinetic constant values for fast-quenching pool of fluorescein molecules on the liposome surface.
[b] Kinetic constants for slow-quenching fluorescein pool.

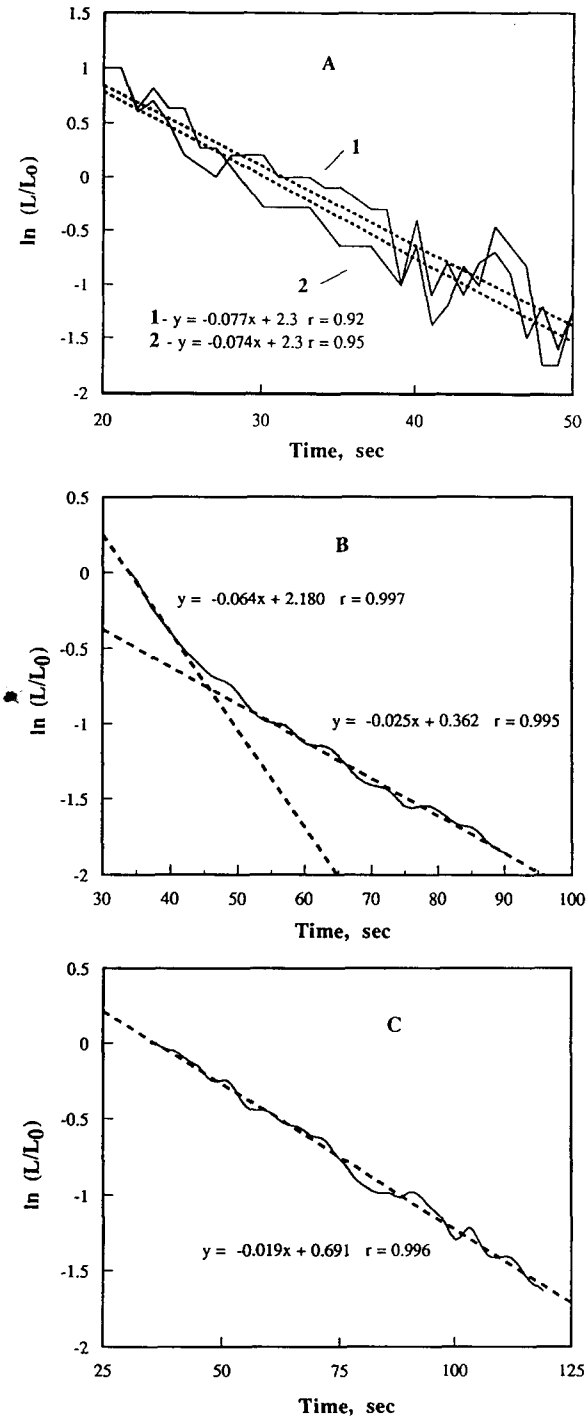

Fig. 9. Linearization of liposomal fluorescein quenching with anti-fluorescein antibody for typical experiments (dotted lines). L/L_0, fraction of free ligand (fluorescein). (A) 'Plain' fluorescein-liposomes (1) and fluorescein-liposomes with 1% mol of dextran (2). (B) Fluorescein-liposomes with 0.2% mol PEG. Two phases on the kinetic curve can be seen – initial fast phase, reflecting the quenching of exposed antigen, and subsequent slow phase, reflecting the quenching of PEG-protected antigen. (C) Fluorescein-liposomes with 1% of PEG. See experimental part for detail.

some-protecting polymers with various molecular sizes, predict possible functional co-existence on the liposome surface of both protective polymer and some other reactive moieties, and improve targeted drug design.

Acknowledgement

This study was funded in part by Sterling Winthrop Pharmaceutical Research Division.

References

[1] Gregoriadis, G. (ed.) (1988) Liposomes as Drug Carriers, Wiley, New York.
[2] Senior, J.H. (1987) CRC Crit. Rev. Ther. Drug Carrier Systems 3, 123–193.
[3] Torchilin, V.P. (1985) CRC Crit. Rev. Ther. Drug Carrier Systems 2, 65–115.
[4] Abra, R.M. and Hunt, C.A. (1981) Biochim. Biophys. Acta 666, 493–503.
[5] Torchilin, V.P., Berdichevsky, V.R., Barsukov, A.A. and Smirnov, V.N. (1980) FEBS Lett. 111, 184–188.
[6] Ellens, H., Mayhew, E. and Rustum, Y.M. (1982) Biochim. Biophys. Acta 714, 479–485.
[7] Allen, T.M. and Chonn, A. (1987) FEBS Lett. 223, 42–46.
[8] Blume, G. and Cevc, G. (1990) Biochim. Biophys. Acta 1029, 91–97.
[9] Papahadjopoulos, D., Allen, T.M., Gabizon, A., Mayhew, E., Huang, S.K., Lee, K.D., Woodle, M.C., Lasic, D.D., Redemann, C. and Martin, F.J. (1991) Proc. Natl. Acad. Sci. USA 88, 11460–11464.
[10] Klibanov, A.L., Maruyama, K., Torchilin, V.P. and Huang, L. (1990) FEBS Lett. 268, 235–237.
[11] Mori, A., Klibanov, A.L., Torchilin, V.P. and Huang, L. (1991) FEBS Lett. 284, 263–266.
[12] Woodle, M.C. and Lasic, D.D. (1992) Biochim. Biophys. Acta 1113, 171–199.
[13] Needham, D., McIntosh, T.J. and Lasic, D.D. (1992) Biochim. Biophys. Acta 1108, 40–48.
[14] Gabizon, A. and Papahadjopoulos, D. (1992) Biochim. Biophys. Acta 1103, 94–100.
[15] Lasic, D.D., Martin, F.G., Gabizon, A., Huang, S.K. and Papahadjopoulos, D. (1991) Biochim. Biophys. Acta 1070, 187–192.
[16] Torchilin, V.P. and Papisov, M.I. (1994) J. Liposome Res. 4, 725–739.
[17] Weissig, V., Lasch, J., Klibanov, A.L. and Torchilin, V.P. (1986) FEBS Lett. 202, 86–90.
[18] Kranz, D. and Voss, E.W., Jr. (1981) Mol. Immunol. 18, 889–898.
[19] Herron, J.N. (1984) in Fluorescein Hapten: An Immunological Probe (Voss, E.W., Jr., ed.), pp. 49–76, CRC Press, Boca Raton.
[20] Wood, C. and Kabat, E. (1981) J. Exp. Med. 154, 432–449.
[21] Weder, H.G. and Zumbuehl, O. (1984) in Liposome Technology (Gregoriadis, G., ed.), 1st Edn., Vol. 1, pp. 79–108, CRC Press, Boca Raton.
[22] Omelyanenko, V.G., Jiscot, W. and Herron, J.N. (1993) Biochemistry 32, 10423–10429.
[23] Delgado, C., Francis, G.E. and Fisher, D. (1992) CRC Crit. Rev. Ther. Drug Carrier Systems 9, 249–304.
[24] Des Cloizeaux, J. and Jannink, G. (1990) Polymers in Solution, Their Modelling and Structure, pp. 63, 280, 539, Clarendon Press, Oxford.
[25] Blume, G. and Cevc, G. (1992) in Abstracts of International Conference '2nd Liposome Research Days', p. SC19, Leiden University, The Netherlands.

[26] Torchilin, V.P., Klibanov, A.L., Huang, L., O'Donnell, S., Nossiff, N.D. and Khaw, B.A. (1992) FASEB J. 6, 2716–2719.
[27] Kurata, M. and Tsunashima, Y. (1989) in Polymer Handbook (Brandup, J. and Himmelgut, E.H., eds.), pp. VII/1–VII/52, Wiley, New York.
[28] Huang, C. and Mason, J.T. (1978) Proc. Natl. Acad. Sci. USA 75, 308–310.
[29] Enoch, H.G. and Strittmatter, P. (1979) Proc. Natl. Acad. Sci. USA 76, 145–148.
[30] Allen, T.M. and Hansen, C. (1991) Biochim. Biophys. Acta 1068, 133–141.
[31] Klibanov, A.L., Maruyama, K., Beckerleg, A.M., Torchilin, V.P. and Huang, L. (1991) Biochim. Biophys. Acta 1062, 142–148.
[32] Blume, G., Cevc, G., Crommelin, M.D.J.A, Bakker-Woundenberg, I.A.J.M., Kluft, C. and Storm, G. (1993) Biochim. Biophys. Acta 1149, 180–184.